Journal of Environmental Chemical Engineering 13 (2025) 117688

Contents lists available at ScienceDirect

Journal of Environmental Chemical Engineering

journal homepage: www.elsevier.com/locate/jece

Life cycle assessment and multi-objective optimization of biogas upgrading using chitosan based composite membranes

Beheshta Dawood [a], Andrea Torre-Celeizabal [a], Cristina Pina-Vidal [b,c], Carlos Téllez [b,c], Marta Rumayor [a], Aurora Garea [a], Clara Casado-Coterillo [a,*]

[a] Department of Chemical and Biomolecular Engineering, Universidad de Cantabria, Santander 39005, Spain
[b] Instituto de Nanociencia y Materiales de Aragón (INMA), CSIC-Universidad de Zaragoza, Zaragoza 50018, Spain
[c] Department of Chemical and Environmental Engineering, Universidad de Zaragoza, 50018, Spain

ARTICLE INFO

Keywords:
Chitosan-cellulose acetate membranes
Chitosan-starch membranes
Biogas upgrading
Multi-objective process optimization
Life cycle assessment

ABSTRACT

Biopolymer membranes, hybridized by non-toxic or renewable fillers are gaining attention on the preparation of membranes for CO_2 separation, providing their flux and mechanical endurance is improved to provide environmental and economic viability as real alternatives in the decarbonization of the chemical industry. Cellulose acetate is the most commonly found natural biopolymer but its preparation needs organic solvents and it is prone to plasticization. Chitosan biopolymer can be produced from fish waste, but its mechanical resistance is limited due to its high hydrophilicity. In this work, chitosan was blended with cellulose acetate or starch, which can also be obtained from biowaste. The membranes were characterized by single N_2, CH_4 and CO_2 gas permeation and also CO_2/CH_4 mixture separation. The CO_2 permeance of CS:ST membranes was closer to commercial PDMS membrane, and the CO_2/CH_4 selectivity of CS:CA membranes was in the range of selective polymer membranes for this application. A sustainability assessment of the membrane fabrication was performed using Life Cycle Assessment with three environmental impact categories (ReCiPe midpoint method): Global warming, energy and materials depletion. A multi-objective optimization model was applied to optimize the process conditions in the simultaneous CO_2 and CH_4 recovery from model biogas feed stream optimal mass and energy balances. The optimized energy consumption for the separation was utilized on the evaluation of the cradle-to-gate environmental performance for the membranes attaining 90 % purity and recovery in CO_2 and CH_4 in the permeate and retentate outlet streams, respectively.

1. Introduction

The application of bio-based technologies in CO_2 separation for the decarbonization and energy transition is a major setting worldwide. Bio-based technologies are increasingly recognized for their potential to maximize the defossilization/decarbonization synergy. Carbon capture and utilization (CCU) is currently accepted as a sustainability approach in the transition to a circular bioeconomy [1]. The circular economy targets closing flows throughout the entire energy and material life cycles by more recycle and reuse efforts. This ultimately should result in increased sustainability [2]. However, considering the entire life cycle there are still gaps in sustainability [3]. In this context, gas separation membrane technology has long been accepted as a sustainable alternative to other separation processes in industrial and environmental applications. However, the membrane modules are mainly based on materials like polyacrylamide or polysulfone and a more environmentally friendly approach would help the transition towards a real circular economy [4,5]. Therefore, the circular economy itself might not be sustainable whereas increasing need for materials and energy is forcing societies to shift not only to renewable sources and environmentally friendly or efficient technologies, but also look to bio-based resources in a circular approach [6].

Biopolymer-based membranes for CO_2 separation offer the unique properties of biopolymers, such as biodegradability and renewability, making them an attractive alternative to conventional petroleum-based polymers, whose benefits go beyond reducing the global warming potential (GWP). These benefits may counterbalance the challenges due to the low scale of fabrication and implementation in CCU applications. These challenges arise from the uncertainty of their long-term stability of performance and cost of fabrication and replacement of membrane

* Corresponding author.
E-mail address: casadoc@unican.es (C. Casado-Coterillo).

https://doi.org/10.1016/j.jece.2025.117688
Received 24 April 2025; Received in revised form 18 June 2025; Accepted 20 June 2025
Available online 24 June 2025

modules. Stability and selectivity of the biopolymers can be overcome by making a mixed matrix membrane (MMM), introducing a small loading of non-toxic or renewable fillers into the continuous biopolymer matrix, providing new mixed matrix membranes with synergic properties with improved permeability and selectivity and mechanical endurance while keeping the processability of the polymers, in comparison with the inorganic fillers cost of fabrication as a continuous membrane. These benefits as well do not have to overcome existing membranes performance, but only approach technical, environmental and economic viability as real alternatives in the decarbonization of the chemical industry in the circular bioeconomy [3].

The understanding of biopolymer-based membranes is also attracting a very recent interest in literature, using increasingly complex phenomenological models [7,8], multi-scale approaches and data-science [9] to predict membrane performance of novel renewable or less toxic materials than the conventional membrane materials in gas separation.

The sustainability of production and consumption patterns is a central topic in the scientific literature and policy debate as social and economic development pressures on the environment are gaining the public sphere [10]. A systematic and holistic tool as life cycle assessment offers the possibility to evaluate the environmental hotspots from materials fabrication to end-of-use, providing the necessary recommendation to produce better energy and waste management policies by decision makers [11]. Application fields of LCA are (i) identification of hot spots within the product's life cycle, (ii) comparison of different products with the same function (functional unit), (iii) comparison of different design, manufacturing, process and materials options within one product's life cycle with the aim of lowering the environmental impacts [12].

Harnessing a green fabrication strategy together with the gas separation membrane performance could be a sustainable remedy both to avoid the amount of oil-based solvents and reactants as well as end-of-life possibilities of the membranes, leading to environmental burdens of the technology [13]. A multi-objective optimization model was established to optimize the process conditions of simultaneous CO_2 and CH_4 separation in biogas upgrading scenarios using chitosan biopolymer membranes hybridized with an ionic liquid of non-reported toxicity and surfactant-free ETS-10 nanoparticle fillers [14]. The environmental life cycle approach has been implied so far by the use of chitosan biopolymer as membrane matrix and non-toxic surfactant free filler on the mixed matrix membranes, or the replacement of toxic organic solvents in cellulose acetate membranes by green solvents [15,16]. Although specific data to evaluate the environmental prospects including detailed production, use, and disposal of membrane units is still scarce in the literature, its interest grows in order to bridge the gaps between laboratory and scale-up of cleaner membrane practices. Common background data are generic or extrapolated thus compromising the accuracy of LCA results [17]. Multi-objective optimization has been applied to the production of green solvents, or the simulation of membrane technology potential in CO_2/CH_4 separation processes, but so far membrane fabrication has not included into the analysis [18].

Therefore, a few papers are appearing in literature using multi-objective optimization for evaluating the process performance and LCA to investigate the environmental feasibility of different emerging technologies. Table 1 collects the papers found in literature using in one way or another LCA to include the membrane fabrication in the environmental assessment of membrane technology, although it should be remarked that the most specific calculations are still reported only for the membrane fabrication and not operation performance [13,19].

In this sense, we agree with [20] in the fact that, when it comes to novel processes, 'bio-based' is not synonymous of environmentally sustainable. They used Aspen Plus to simulate different separation process scenarios. The system boundaries of the LCA study were the process units in the process simulation. This was the approach followed by Luis et al. [21] to compare the performance of a hybrid purification process with the conventional stand-alone distillation. The most frequent impact categories collected in Table 1 can be divided in four categories related to human health (HH), ecosystem quality (EQ), climate change (CC) or resource depletion (RD). The energy consumption is the most common way of quantifying the environmental impact thus the process modeling results in the determination of the cumulative energy demand (CED) by the membrane production process [22]. Markewitz et al. [23] used LCA to analyze the environmental impact of BSCF membrane modules in the O_2 separation for oxyfuel power generation, including the membrane production as well as the performance data on the assessment. Likewise, Khaki et al. [24] used CED to introduce the CO_2 capture capacity of three different polymer membranes whose inputs and outputs in membrane fabrication were the only entries of the Life Cycle Inventory taken into account. As observed in Table 1, the conventional approach of these studies is either devoted to the environmental assessment or the process optimization. Recent works have begun implementing the environmental impact of a membrane process configuration into the multi-objective optimization [25].

Regarding the sustainability assessments of membrane fabrication and operation in literature, Giordano et al. [26] used the LCA tool to compare non-commercial high permeability membranes based on PIM-1, with commercial CO_2 capture membranes and chemical absorption, reflecting in the limitations of conventional polymers to be implemented as sustainable alternative technology. Mixed matrix membranes, combining the synergistic properties of a highly novel filler into a known polymer matrix, has been widely studied in literature. Tuning of permeability and selectivity was attempted by small loadings with commercial 4 A zeolite, which is a commonplace nanoporous available filler for the design of gas separation MMM [30]. The otucome of biopolymers in membrane technology has boosted the use of LCA tool to evaluate the environmental assessment of membrane fabrication in comparison with conventional membrane materials [19,22], especially cellulose acetate, which is fabricated from the most abundant polysaccharide in nature (cellulose fiber) [15] and also with high potential to incrase the viability of biogas upgrading plants through membrane technology [31]. Chitosan, or poly[β(1→4)-2-amino-2-deoxy-d-glucopyranose] is a linear polysaccharide obtained from the deacetylation of chitin, an abundant natural polymer cheap and present in renewable resources including fish food waste. Together with cellulose acetate, CS is one of the most studied biopolymers for CO_2 separation membranes [32]. The lack of mechanical resistance can be overcome by blending with other polymers and hybridizing with small amounts of porous particles into a MMM, which may be achieved by focusing on the sustainability of the filler dispersed phase in the CS continuous matrix [33]. The study of the structure-property relationship effect of chitosan and film forming derivatives is relevant to the separation performance. Multi-objective optimization providing feedback to advance in membrane and process design have been evaluated in our group [14,29]. Recently, an integrated approach evaluating the environmental and economic performance of the production of UiO-66-NH_2 adsorbents with affinity for CO_2 capture [26] included in PIM-1 polymers to study their potential in membrane separation [13] considering lab-scale synthesis first and then applying LCA to hypothetical pilot-scale productions to evaluate the overall environmental impact.

The novelty of this research deals on the combination of environmental analysis of the fabrication of new CO_2-selective chitosan-based membranes with the optimization of these membranes' performance in the simultaneous recovery of CO_2 and CH_4 from a typical biogas effluent from anaerobic digestion plant. This way, the optimized energy consumption and membrane are introduced in the LCA model to evaluate the environmental hotspots of the cradle-to-gate system. This methodology provides a flexible approach that includes scalability factors and the consideration of the complexity of supply chains, such as an accurate accounting of the biological sources and processing methods. In addition, chitosan -based membranes are blended with cellulose acetate (CA) and starch, CA is the most common biopolymer in CO_2/CH_4

Table 1
Scientific publications dealing with LCA and multi-objective studies using membranes.

Ref.	Process	Multi-objective optimization	LCA scope	Functional unit	Impact factors**
[19]	Preparation of PVA-based porous supports using aqueous solutions	N.A.*	LCA cradle-to-gate, with Simapro and eco-invent 3 databases	1 m2 membrane surface area	11 CML impact categories: ADPE, ADPF, ODP, TEP, GWP, HTP, FWAEP, MAEP, POP, EP, AAP
[17]	CO_2/N_2 separation by chitosan-based MMMs	N.A.	The potential of bio-based membranes in CO_2 separation	1000 m^2 of permeation area	GWP, ODP, AC, EUT, EUF, EUM, HTC, HTNC, ECFM, LU, WU
[23]	BSCF OTM for ASU in oxyfuel power generation	Needed [25]	Environmental assessment of membrane fabrication and performance	1 kWh electricity produced	GWP, AP, EP, POCP, HTP, MAEP, FAEP
[26]	CO_2 capture post-combustion process	Needed.	Environmental impact comparison of CO_2 capture using three different configurations of 2-stage membrane unit	1 t CO_2 from exhaust flue gas	CML-IA baseline method for 11 impact categories: ADPE, ADPF, ODP, TEP, GWP, HTP, FAEP, MAEP, POP, AP, EP.
[24]	CO_2 capture by high permselective polymer membranes based on PAN, PVIM P(AN-co-VIM)	Cumulative energy demand (CED) method	Specify the environmental impacts of CO_2 separation (EF)	CO_2 adsorption capacity	ADP, GWP, ODP, HTP, FAEP, MAEP, TEP, POP, AP, EP
[27]	CO_2 adsorption by UiO−66-NH_2 adsorbents vs MEA absorption	TEA (capital cost and operating cost, space-time yield STY)	Comparison of solvothermal and aqueous synthesis of UiO−66-NH_2 adsorbents	1 MWh electricity exported (t CO_2eq/ MWh)	GWP
[21]	Separation of methanol/THF	Design of hybrid distillation-pervaporation process: energy requirements	Compare environmental impact of hybrid with stand-alone distillation process	1 kg solvent	ReCiPe 2008 midpoint categories: GWP, ODP, TEP, FEP, MAEP, HTP, POFP, PMP, TEP, FAEP, MAEP, ionising radiation, agricultural land occupation, urban land occupation, natural land transformation, water depletion, MRD, FD.
[20]	Separation of 2,5-furandicarboxylic acid by crystallization (A) and distillation (B)	Process modeling by Aspen Plus v9 considering two scenarios of product purification	Comparison of scenarios. Gate -to-gate	1 kg/h FDCA	GHG, NREU
[28]	CA UF membrane fabrication	Parametrized model to obtain material and energy flows from operating conditions	Evaluate environmental hotspots of membrane fabrication	1 m^2 filtration surface in the HF module	ReCiPe endpoint: LU, GWP, FD, natural land transformation
[22]	Cellulose membrane manufacturing by electrospinning	N.A.	CED, IMPACT2002 +	1 batch electrospun membrane	15 ReCiPe midpoint categories: AAP, AEP, AEUP, GWP, IRP, MEP, HCTP, HNCTP, LUP, NREP, OLDP, RIP, ROP, TANP, TEP
[13]	Production of UiO−66-NH_2-PIM MMMs	Techno-economic analysis, CED	Cradle-to-gate	1 kg dry basis product	GWP, PMFP, TAP, FEP, HTP, WDP
[14, 29]	specific energy consumption, membrane area needed (material requirements)	Chitosan-based membranes for biogas upgrading	Techno economic analysis on purity and recovery targets for retentate and permeate streams	N.A.	N.A.

* N.A.: not available.

** AD: Abiotic depletion; GWP: Global warming; ODP: ozone layer depletion; HTTP: human toxicity; FAEP: Freshwater aquatic ecotoxicity; MAEP: marine aquatic ecotoxicity; TECP: terrestrial ecotoxicity; POP: photochemical oxidation; AP/ACI: acidification; EU/EP: eutrophication; FU: land use; FD: fossil fuel depletion; RINP: respiratory inorganics; NREU: non-renewable energy; MRD: mineral resources use; AC: acidification; EUT: eutrophication, terrestrial; EUF: eutrophication, freshwater; EUM: eutrophication, marine; HTC: human toxicity, carcinogenic; HTNC: human toxicity, non-carcinogenic; ECFM: ecotoxicity, marine; LU: land use; WU: water use.

separation, and starch another biopolymer that can be obtained, such as chitosan, from biowaste.

2. Methodology

2.1. Experimental section

2.1.1. Materials

Chitosan (CS, from crab shells), starch (ST, potato starch), cellulose acetate (CA, 30 molecular weight) and zeolite A nanoparticles (Molecular sieves 4 A) were purchased from Sigma-Aldrich (Spain). Acetic acid glacial (CH_3COOH, M=60.05) was obtained from PANREAC (Spain), and deionized water was produced using Elix® technology. Polyethersulfone (PES) supports of 0.1 and 0.2 μm pore size were provided by Micromeritics (PALL, France), was used to provide with further mechanical robustness to the composite membranes.

2.1.2. Membrane preparation and characterization

Membranes were prepared from equimolar blends of CS:CA and CS:ST, from CS 1 wt% solutions in 1 wt% acetic acid/H_2O, 1 or 4 wt% ST dissolved in water at 90ºC and 1.5 wt% CA in acetone. In a typical membrane preparation, the biopolymer solution was prepared by dissolving equal amounts of CS and ST (0.5 g each) in 1 wt% aqueous acetic acid under reflux at 90°C for 24 h with constant stirring, followed by vacuum filtration to remove impurities. Blends of CS:ST were prepared from 1 and 4 wt% starch solutions, in order to observe the effect on the membrane robustness and the selective membrane thickness, but the CS and ST were in an equimolar base ratio in all cases. For the CS:CA blends, the polymers were mixed from the previously prepared solutions, under stirring at room temperature for 24 h, also in an equimolar basis with respect to CS. Biopolymer membranes were fabricated via solution casting onto the PES support, and subjected to solvent evaporation at room temperature and further dried at 50ºC in oven without convection. The resulting membranes were peeled off for further analysis.

In order to try to tune up the swelling resistance and selectivity of the CS-based membranes, mixed matrix membranes were prepared in a similar way as reported elsewhere [8,33] using a commonplace nanoporous commercial zeolite 4 A as filler. Typically, a dispersion of zeolite nanoparticles in 2 mL H_2O was added to each CS polymer blend solutions, to make up for a total loading ratio of 2.5 and 5 wt% with respect to the total solid polymer matrices. The nanoparticles were dispersed in 6–8 mL polymer solutions and stirred for homogenization.

2.1.3. Characterization of the membranes

The thickness of the prepared membranes was measured using a Mitutoyo digimatic micrometer (IP 65, Japan) with an accuracy of 0.001 mm. Measurements were taken at five points across the effective membrane area, and the average thickness along with the standard deviation was calculated.

Thermal stability was evaluated through thermogravimetric analysis (TGA) using a Shimadzu DTG-60H thermobalance in air and nitrogen atmospheres (50 $cm^3(STP) \cdot min^{-1}$). Membrane samples (1–5 mg) were placed in alumina pans and heated at a rate of 10 ºC/min up to 650 ºC.

Attenuated Total Reflectance Fourier-Transform Infrared Spectroscopy (ATR-FTIR) was performed using a Perkin Elmer Spectrum 65 FT-IR spectrometer to study molecular interactions on the membrane surface. The absorbance of membranes with varying compositions was recorded in the 500 cm^{-1} range.

Scanning electron microscopy (SEM) images of the membrane cross-section were captured with an Inspect F50 model scanning electron microscope (FEI, operated at 10 kV).

X-ray diffraction (XRD) membrane patterns were collected in the range $2\theta = 2.5 - 40^{o}$ using a scanning rate of 0.01° s^{-1} in an Empyrean PANalytical diffractometer (Malvern Panalytical) using a CuKα radiation ($\lambda = 1.5406$ Å).

2.1.4. Gas permeation measurement

The performance of the mixed matrix composite membranes was characterized using a custom-built gas separation setup reported elsewhere [33]. Membranes were cut to an effective area of 15.55 cm^2 and mounted in a stainless-steel module comprising two compartments. The membrane was positioned over a microporous stainless-steel disk support with a pore size of 20 μm and sealed with Viton rings to prevent leakage. Pure gas streams of nitrogen (N_2), methane (CH_4), and carbon dioxide (CO_2) were sequentially introduced in that order into the module to evaluate gas permeation at 20ºC and 4 bar feed pressure. The feed flow rate was set at 50 $cm^3(STP) \cdot min^{-1}$ by mass flow controllers (KOFLOC 8500, Sequopro S.L., Madrid, Spain). Each permeation experiment lasted for at least 1.5 h for every individual gas under investigation. The permeate flow rate was quantified using a bubble flow meter installed at the outlet of the membrane module. Mixed gas experiments were measured in the same plant by adjusting the CO_2 and CH_4 flowrate at the required composition, 50/50 (v/v%) or model biogas (35/65 v/v%). The permeate stream was finally measured using a BIOGAS5000 analyzer (Fonotest, USA).

The gas permeance is a measure of the pressure-normalized flux of the gas through the membrane, calculated by Eqn 1 and expressed in GPU,

$$\left(\frac{P}{\delta}\right)_i = 10^{-6} \cdot \frac{Q_p}{\left(p_r - p_p\right) \cdot A} \quad (1)$$

where i denotes each gas molecule (N_2, CH_4 or CO_2), δ, the membrane thickness (cm), Q_p, the permeate flowrate measured at the exit of the plant ($cm^3(STP) \cdot s^{-1}$), A, the effective membrane area for permeation (cm^2), p_r and p_p, the retentate and permeate pressure, respectively (cmHg). P is the intrinsic permeability of the membrane material for each gas (cm^3(STP) cm cm^{-2} $cmHg^{-1}$ s^{-1}). The permeability, when calculated, is given in Barrer (1 Barrer = $10^{10} \cdot cm^3$(STP) cm cm^{-2} $cmHg^{-1}$ s^{-1}).

The ideal selectivity of the membrane is determined by the ratio of the permeability of two individual gas permeation fluxes, as

$$\alpha = \frac{(P/\delta)_i}{(P/\delta)_j} \quad (2)$$

Upon mixed gas separation experiments, the separation factor of the membrane unit is calculated by Eqn 3 from the mass fractions of i and j in the permeate (y) and retentate (x), as

$$S.F. = \frac{\left(y_i / y_j\right)}{\left(x_i / x_j\right)} \quad (3)$$

Since we have observed in previous works that the intrinsic selectivity of the membrane material in pure gas experiments and the separation factor in mixed gas experiments at the relatively low pressure of this work have similar values, we will use the values of ideal selectivity from Eq. (2) in the results and discussion section.

2.2. Life Cycle Assessment (LCA)

In this study, the methodological framework outlined by the International Organization for Standardization (ISO) 14040–44 [34,35] was employed to conduct a LCA. This methodology follows the systematic steps: goal and scope, life cycle inventory life cycle impact assessment and interpretation.

The goal of this LCA is to evaluate the environmental impacts associated to the biopolymer membrane fabrication and operation. The functional unit (FU) was defined as 1 m^2 of membrane surface area to compare the relative environmental impacts of the membrane fabrication, and 1000 $Nm^3 \cdot h^{-1}$ to assess the environmental impacts in the optimized CO_2/CH_4 separation in a large-scale biogas upgrading plant capacity. This choice facilitates the comparison with existing literature

and ensures consistency in evaluating environmental impacts.

The analysis was performed from a cradle-to-gate perspective, as illustrated in the schematic diagram in Fig. 1. System boundaries include raw material extraction, the production of polymers, solvents and reactants for the fabrication of membranes (*e.g.* chitosan from shrimp shells or heating-drying steps upon membrane fabrication).

The Life Cycle Inventory (LCI) step involved gathering both primary and secondary data. Primary data on membrane fabrication and permeation testing, were taken from the laboratory data as explained in the previous section. Secondary data, representing the background processes which complement the primary data to complete the assessment, were obtained from the literature on chitosan and starch fabrication from food waste, namely, chitosan shrimp shells and potato peels, respectively [36,37]. For the rest of the secondary data, the Ecoinvent v3.11 database [38] was used, with the geographical context set to Europe (EU-28) or global (GLO) depending on availability. This approach allowed the retrieval of existing data aligned with the objectives of the study, ensuring that the background processes were accurately represented in the LCA framework. The calculations for energy and material consumption upon membrane fabrication are based on the experimental data, with a scale-up approach applied following the methodology outlined by [39]. According to this, the heat and stirring energy consumption (Fig. 1) aimed to dissolve starch at 363 K under agitation at 300 rpm for 24 h can be calculated by Eqn 4.

$$Q_{heat} = C_p \cdot m_{mix} \cdot (T_r - T_0) \quad (4)$$

where Q_{heat} is the energy to reach the set point temperature (J), C_p the specific heat capacity of the main solvent (J $kg^{-1} \cdot K^{-1}$), m_{mix}, the mass of the mixture (kg), T_r, the heating temperature (K) and T_0 the starting temperature, usually 294.15 K.

Likewise, the energy consumption upon stirring is calculated assuming that the density of the mixture (ρ_{mix}) is the ratio of the m_{mix} and the volume of the mixture (V_{mix}), and assuming an axial flow impeller, hydrofoil type is used for stirring. Then we can use the following equation,

$$E_{stir} = \frac{N_p \cdot \rho_{mix} \cdot N^3 \cdot d^5 \cdot t}{\eta_{stir}} \quad (5)$$

where N_p is a power dimensionless number according to the theory of dimensional analysis, specific to a certain type of impeller and constant at turbulent flow. For this study, stirring at turbulent flow is considered, so the power number is constant in Eqn 5. N, the rotational speed of the agitator, (s^{-1}), d, the impeller diameter (m), t, the time duration for the stirring process (s) and η_{stir}, the efficiency of the stirring.

The drying of the membrane involves evaporation of the main solvent, *i.e.* water, in this work. The calculation of the energy consumption for drying the membranes is carried out by Eqn 6, considering the energy required to raise the temperature of the liquid to boiling temperature, or 373.15 K in this case, and the enthalpy for the evaporation of water at 373.15 K, assuming that 80 % of the water bound in the membrane matrix is evaporated.

$$Q_{dry} = \frac{C_p \cdot m_{liq} \cdot (T_{boil} - T_0) + \Delta H_{vap} \cdot m_{vap}}{\eta_{dry}} \quad (6)$$

where Q_{dry} is the heat necessary for drying (J), m_{liq}, the mass of liquid of the solution (kg), T_{boil}, the boiling temperature of the liquid (K), ΔH_{vap}, the evaporation enthalpy of water (solvent) (J $kg^{-1} \cdot K^{-1}$), m_{vap}, the mass of the liquid that is evaporated (kg), η_{dry}, the drying efficiency.

After collecting the Life Cycle Inventory (LCI) data, the next step is to evaluate environmental impacts using the Life Cycle Impact Assessment (LCIA) methodology. This involves classifying emissions and resource use into the selected impact categories and characterizing them into standard units for comparison. The life cycle inventories of the fabrication of the chitosan blend composite membranes and mixed matrix membranes based in experimental and literature data are collected in the supplementary information. The ReCiPe Midpoint (H) method [40] was applied to calculate these impacts, ensuring standardized and comparable results. The environmental impacts account for raw materials, solvents, and energy and heat consumption throughout the manufacturing. The analysis focuses on key environmental indicators, including climate change (GWP), energy resource consumption (non-renewable, fossil; FD), and material resource depletion (metals and minerals; MD), relevant to identify the hotspots of the membrane synthesis in comparison with the synthesis of a fossil-fuel based commercial membrane. Then, the selected midpoint categories include climate change (GWP), energy resource consumption (non-renewable, fossil; FD), and material resource depletion (metals and minerals; MD). The influence of location, transportation and end of life falls outside the scope of the current study which is focused on the separation process itself. The analysis was performed in Excel and openLCA software [41] with comparable results.

2.3. Multi-objective process optimization

In the membrane-based separation of CO_2, N_2 and CH_4 from different sources, the purity and recovery of permeate and retentate streams are crucial to determine the technical viability of the process. However, in order to analyze the potential scalability, economic cost and energy consumption are critical indicators of technical feasibility. A diagram of the research strategy is shown in Fig. 2, summarizing these objectives and the steps proposed in the methodology applied to biogas upgrading.

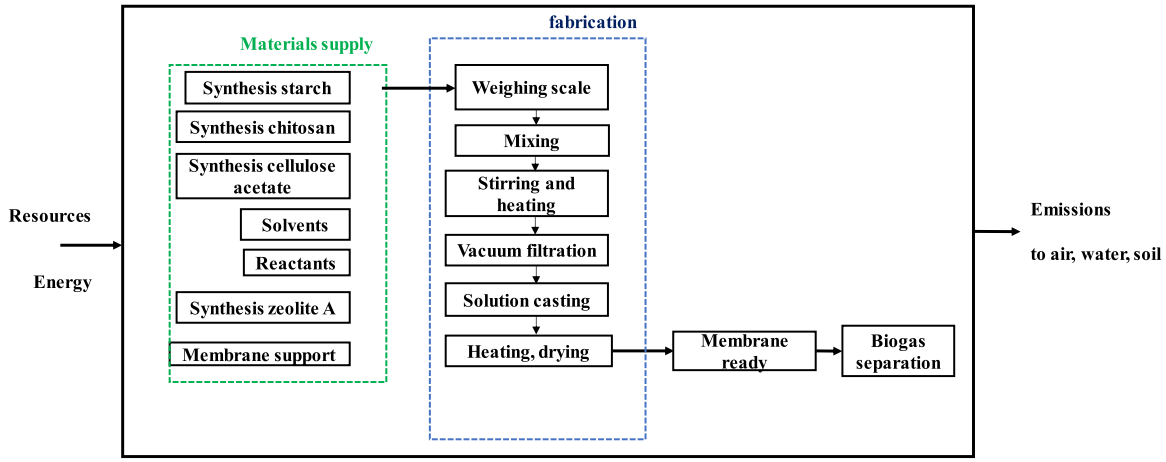

Fig. 1. LCA system boundary of membrane module fabrication model.

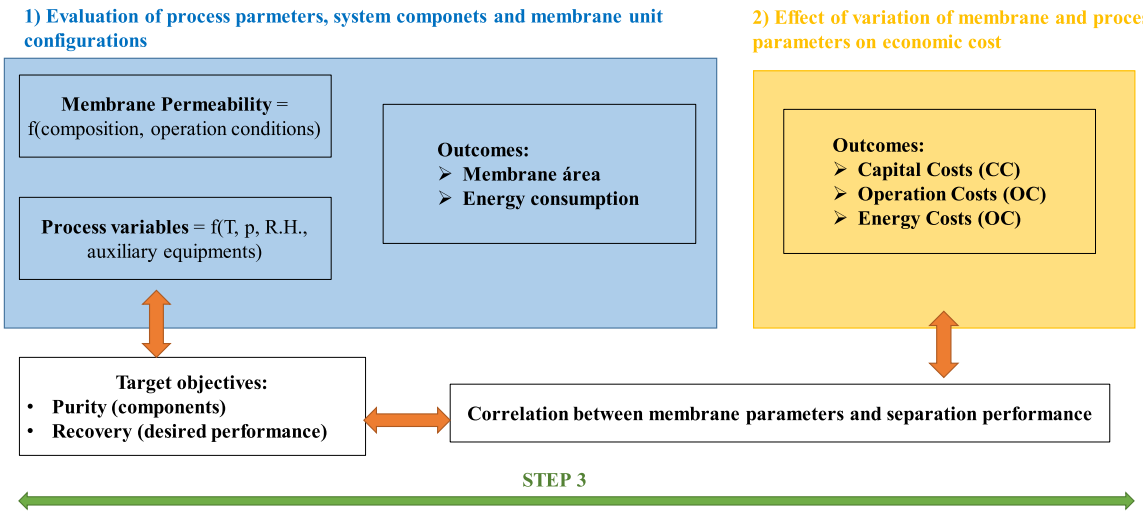

Fig. 2. Schematic diagram of the research strategy for the techno-economical optimization of a membrane separation process, involving membrane and process design. Adapted from Abejón et al. [29].

Multi-stage configurations are needed to achieve a high trade-off in purity and recovery in gas separation processes. The requirement of multiple membrane stages for effective gas separation processes implies the design of membrane networks and interconnections in superstructures, to be solved using different programs or commercial packages of mathematical programming for optimization. Based on the experience of previous works [29,42], we propose a 3-stage membrane network for the separation of CO_2 and CH_4 from a typical biogas composition, shown in Fig. 3. This setup consist of 3-stage membrane units in series as regards the CO_2-enriched permeate line, while the retentate is obtained from the mixing of the retentate outputs of all the membrane units, to recover simultaneously CO_2 and CH_4 from the biogas stream. The process optimization procedure applied to the separation of CO_2 and CH_4 is based on the maximizing purity and recovery of CO_2 in the permeate outlet, with values ≥ 90 % as target objectives of the separation performance.

Membrane units are described by a cross-flow membrane model based on a cell-in-series assumption, where the membrane is divided into 100 equal-sized cells. The transport mechanism across the membrane is described by the solution-diffusion model, with the partial pressure difference as driving force [42].

Compression units, compressors and associated heat exchangers, are included in the permeate line to set the feed pressure and temperature at the inlet of each membrane unit, as well as in the feed line to the process. The use of an expander for the CH_4 enriched product is also included in the calculation of total process costs.

The three-stage process is modelled as a custom-built programming of a nonlinear problem using GAMS software, which is one of the leading tools for algebraic modelling and optimization [43,44]. It consists of a language compiler and a stable of integrated high-performance solvers (GAMS Development Corp., GAMS Software GmbH).

Following the procedure detailed in previous studies [14,29,42], the formulation in mathematical terms is given by Eqn 7 as

$$\max f(x) \tag{7}$$

$$\text{s.t. } h_m(x) = 0, \forall\, m$$

$$g_n(x) \leq 0, \forall\, n$$

$$x \in \mathrm{R}^n,\ X_L < x < X_U$$

where the objective function $f(x)$ is defined as the sum of purity and recovery of components from the feed stream to the separation process, and subject to equality constraints $h_m(x)$ such as the material balances, separation process design equations, cost equations and correlations used in the economic analysis; as well as inequality constraints $g_n(x)$ to specify the lower and upper bound of operational variables.

The resulting NLP problem is solved in GAMS (v39.3.0) employing the CONOPT3 solver. Fig. 3 includes the main fixed and calculated variables at each stage and the multistage process outlet for CO_2 and CH_4 separation and recovery. The input parameters correspond to the characterization of the membrane related to the separation performance, given by the CO_2 permeance and the selectivity of the CO_2/CH_4 pair. Fixed variables are those corresponding to the feed stream (flowrate, composition and pressure), as well as the pressure ratio at which each

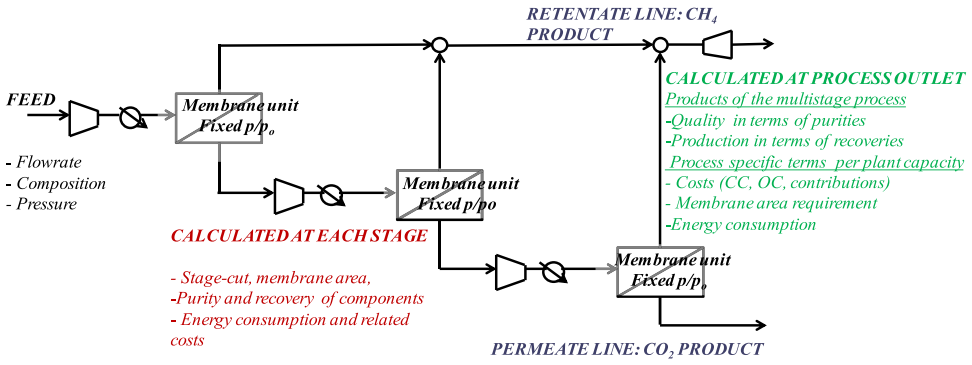

Fig. 3. Flowsheet of a 3-stage membrane separation systems for the simultaneous separation of CO_2 and CH_4 from biogas. Summary of variables calculated at each stage and the multistage process outlet.

membrane unit operates (p/p_o). The calculated variables are the related to the outlet streams at each stage (flowrate, composition, as well as purity and recovery of both components, CO_2 and CH_4); as well as the operation of membrane units, in terms of the membrane area required for the separation in each stage. The stage-cut variable, defined as the ratio of the permeate flowrate and the feed flowrate, is highlighted as a decision variable to achieve product specifications, with values $\geq$ 90 % purity and recovery of CO_2 in the permeate outlet, as target objectives of the separation performance. Boundary conditions applied to stage-cut are 0.05–0.95,

The economic evaluation of the separation process is performed to estimate the total costs (TC) and its specific term per plant capacity ($TC_{specific}$), referred to the feed flowrate to the separation process (Q_{Feed}) and taking into account the on-stream factor (OSF, value 0.96) [29]. Total Costs are calculated from the contributions of cost terms related to capital costs (CC), operational costs (OC), and the cost of CH_4 loss in the permeate at process outlet (LSC), according to equations Eqn 8, 9, 10 and 11.

$$TC = CC + OC + LSC \tag{8}$$

$$TC_{specific} = \frac{(CC + OC + LSC)}{Q_{Feed} OSF} \tag{9}$$

$$FC = MEC + TUC + HEC + COC \tag{10}$$

$$OC = MRC + UC + LC + IC + MC \tag{11}$$

The capital costs (CC) are mainly based on the fixed costs (FC, Eq.10) corresponding to the investment in equipment, with the contributions of membrane modules (MEC), compressors (COC), heat exchangers (HEC) and turbines (TUC). Aspects such as project contingency and start-up costs are also included in capital costs.

The operation costs (OC, Eq. 11) are based on the consumption of the corresponding resources in terms of utilities (UC, electricity and cooling water), membrane replacement (MRC) and labor (LC); while the maintenance and insurance costs (MC, IC) are functions of the total capital costs.

Table S1, in the Supporting Information, details the costs equations and related terms in the economic evaluation of the three-stage membrane separation process. The Chemical Engineering Plant Cost Index (CEPCI) is used, and those corresponding to the performance of the equipment are also referenced.

The results of process performance are then summarized per plant capacity (considering the feed flowrate basis), in terms of the total membrane area requirement ($m^2 \cdot (Nm^{-3}\, h^{-1})$), the specific total cost (€ Nm^{-3}), as well as the contributions of cost terms in fixed and operating costs, and the specific energy consumption (kWh Nm^{-3}).

3. Results and discussion

3.1. Membrane characterization

The membranes are experimentally characterized regarding thickness, thermal and microstructure properties among other techniques, that influence the morphology, *i.e.,* thickness and homogeneous dispersion of the components in the membrane matrix and has an effect on the gas permeation performance. For the CS:ST unsupported membrane, the thermogravimetric analyses in Fig. 4 show the two degradation steps characteristic of chitosan and potato starch composite materials, corresponding to the loss of bound water (50–120ºC) and the polymer chain degradation (mainly between 498 and 623 K) [45,46]. When the CS:ST membrane is deposited on the PES support, the weight losses of CS:ST previously mentioned are maintained but now there is a predominant weight loss starting at 748 K, which corresponds to the degradation of PES. CS:CA and CS:ST supported membranes degrade at similar temperatures, although with CA it seems that the degradation of

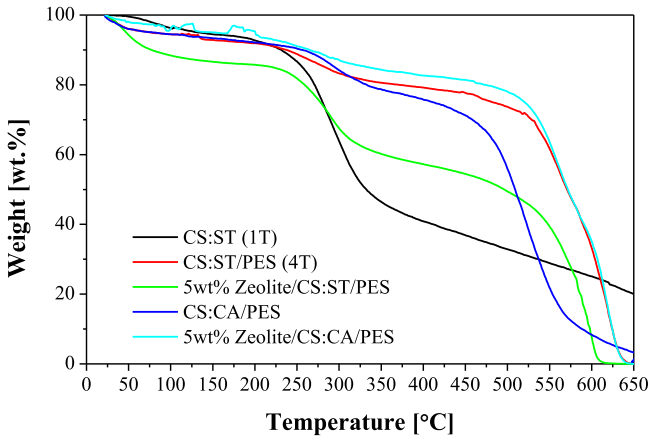

Fig. 4. TGA of the CS:blend composite membranes prepared in this work.

PES is slightly accelerated. The thermal stability seemed improved by the use of 4 wt% ST solution instead of 1 wt%, since the degradation temperatures are slightly shifted to higher values upon blending. The ST was more hydrophilic than CS, and thus these observations may be masked by the water sorption even after weeks after membrane testing.

More on this water uptake properties may be discerned in Fig. 5. The ATR-FTIR spectra CS:ST composite membranes reveal the characteristic bands of chitosan and starch dominate the scenery, as expected given the low zeolite 4 A ratio used in this work. The broad OH- band at around 3335,8 cm^{-1} due to the stretching of -OH groups in the biopolymers diminishes with increasing zeolite loading, together with the bands at around 1648 an 1373 cm^{-1} assigned to the amide I band and amide II [47]. This responds to the hydrophilic character of this zeolite that partially adsorbs water in its porous framework [48] and contributes to the faster drying of the composite membrane upon preparation [49]. The weakening of the polymer peaks hints to the adhesion between the zeolite 4 A and the CS:ST blend matrix in agreement with the broad diffraction observed in the XRD patterns (Figure S1 of the Supplementary information) and the thermograms of Fig. 4, leading to a defect-free membrane layer. A small band at 660 cm^{-1} appears on the CS:CA mixed matrix membranes that may be attributed to the presence of the zeolite filler.

More insight of the homogeneity of the CS:ST top layer and the compatibility with the porous PES support can be discerned in the electron microscope images of Fig. 6. Fig. 6**(d)** is a larger magnification image of Fig. 6**(c)** to see the compatibility between the CS:ST top layer and the support. Furthermore, the MMM shows good adhesion between the zeolite and the polymer blends in the selective layer.

Using SEM micrographs, although the cut may make measurements difficult, the thickness of the selective layer can be estimated after gas permeation tests. The thickness of the CS:ST selective layer prepared with 4 wt% ST solution in the CS:ST(1:1) blend is approximately 3 μm, with a value for the MMM. The membrane prepared with 1 wt% ST shows a greater thickness of 6 μm. The thickness values of the top layers observed by SEM images are nevertheless lower than the thicknesses measured in the laboratory before the gas permeation experiments (see Table 2). These differences could be due to inaccuracies between both measurement methods and the compaction occurring during the gas separation measurements [50].

Table 2 collects the average results of the CS blend composite membranes regarding CO_2 permeability and CO_2/CH_4 selectivity. CS:CA blend membranes observed CO_2/CH_4 selectivities commonly reported for CA membranes in literature, at the cost of a lower permeance. Cellulose acetate membranes generally have a CO_2/CH_4 selectivity of 35–40 in single CH_4 and CO_2 permeation tests, while thin membranes measured with binary CO_2/CH_4 mixtures are usually reported at selectivity values of 15–20 [51], because of the high tendency of CA to

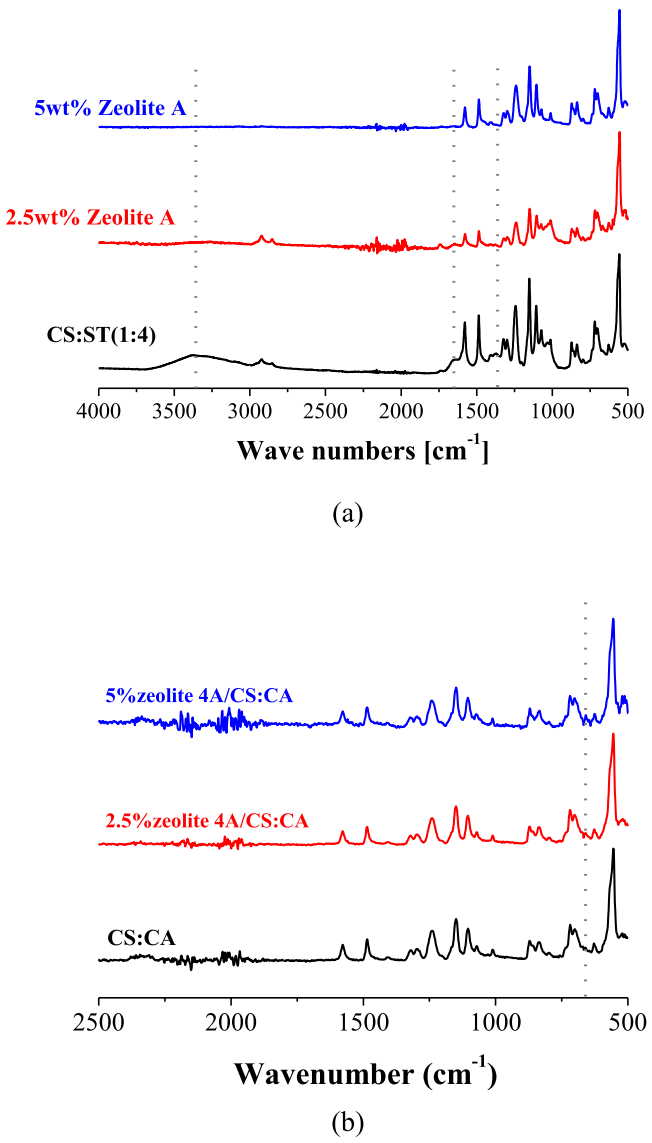

Fig. 5. ATR-FTIR of the CS-based composite membranes where CS was blended with ST (a) and CA (b), respectively.

undergo plasticization. This phenomenon was not observed in our work at pressures up to 5 bar, but the permeability was low even though it was slightly improved by the addition of the porous zeolite 4 A filler, with affinity to water vapor and CO_2 streams. On the other hand, CS:ST composite membranes showed a permeance closer to the commercial PDMS membrane at high selectivities.

We will analyze the sustainability and scalability of the fabrication and the scalability for biogas upgrading in the following sections.

3.2. *Impacts of membrane fabrication*

This section shows the results of the Life Cycle Assessment (LCA) conducted for the fabrication of the CS-blend membranes in Table 2. The experimental mass and energy inputs observed upon membrane fabrication in the laboratory are collected in Table 3 and Table 4 for CS:CA/PES, and CS:ST/PES membranes. The energy consumption upon membrane fabrication was calculated as explained in Section 2.1.2 by Eqs. (4)-(6). The synthesis of chitosan was estimated as reported in literature to account for the fabrication of CS from fish residues. Likewise, for the synthesis of starch from potato peels the methodology of Fronza et al. [52] was followed.

The reference scenario in this case is the fabrication of the commercial PDMS-base membrane. The material and energy input flows were calculated from the composition and structural information provided by the supplier, estimated for a membrane size equivalent to the CS:blend membranes prepared in the laboratory. The main parameters are given in Table 5.

Yet few LCA studies on membrane-based systems address membrane fabrication so it is difficult to compare the inventory the environmental impacts of the fabrication of the CS-based composite membranes in this work and the commercial fossil based PDMS membrane characterized as reference. The environmental impacts of the CS-blend composite membranes to global warming are dominated by the fossil energy consumption stages upon membrane preparation, quantified by Eqs. (4)-(6) after Piccinno et al. [39]. While in the reference situation, the ReCiPe midpoint scores for the fabrication of 1 m^2 conventional membrane reaches nearly 11 kg CO_2-eq, and 7 kg oil-eq, respectively, in agreement with literature [28], the CS:CA based composite membranes give 5.2 kg CO_2-eq and 2.7 kg oil-eq, and the substitution of organically dissolved CA by hydrophilic starch, 1.9 kg CO_2-eq and 0.6 kg oil-eq. Much lower is the impact due to the fossil-based material resources of the preparation of the commercial membrane, except for the background processes associated with the obtention of chitosan polymer from fish waste, *i.e.,* the NaOH and HCl needed for the extraction and neutralization of chitin from shrimp shells and the NaOH for the deacetylation of chitin to chitosan [36], or the acetone used to dissolve cellulose acetate before blending.

The environmental hotspots of membrane fabrication are highlighted by the relative contribution of material and energy flows in Table 3 to the different environmental impact categories in Fig. 7. The flows with values of the environmental indicators lower than 0.01 kg equivalent per functional unit are not taken into account in this discussion according the cut-off criteria. The functional unit for the evaluation of the sustainability of membrane fabrication is 1 m^2 surface area, to allow comparison with the literature. The major contributions are due to the polymers and solvents used, for the commercial membrane and also chitosan, because the production of HCl and NaOH still relies in energy intensive chemical processes. Also, the acetic acid that has been added to dissolve the chitosan in the membrane fabrication is derived from fossil resources. This agrees with literature. Among the first reports on LCA for membrane module fabrication were Lawler et al. [53], who observed that the membrane sheet in the whole RO module was responsible for the largest environmental impacts, due to the polymers and solvents used. CS:CA composite membranes were also prepared in our laboratory in an effort to improve both the mechanical and water-swelling resistance of CS and the plasticization tendency of CA. CA is not soluble in aqueous mixture, so acetone was employed in opposition to traditional organic solvents with environmental or human toxicity as studied by Prézélus et al. [28]. This allows us to confirm the effect of the fossil-derived organic solvents on the environmental impacts of membrane fabrication, because the impact of acetone used to dissolve CA before blending with CS surpasses that of the acetic acid used to facilitate the aqueous solution of CS. In fact, the contribution of acetone to GWP is equivalent to that of n-hexane in the commercial membrane. The impact of the CS and CA polymer fabrication to GWP is much lower than the PDMS used in the fabrication of the commercial membrane. In a future work, given the difficulty of dissolving CS in non-protonated form, acetic acid substitution by less intensive acids such as citric or lactic acid will be considered [54]. Likewise, the advancements in the use of green solvents in conventional gas separation polymer, as PEBAX [55] can be also applied to reduce the significant impact of acetone in the CA solution preparation [56]. The impact categories selection for this study agrees with the study of Prézélus et al. [28] for assessing the sustainability of CA membranes.

The contribution to overall impact categories of the energy consumption calculated for the scale-up of membrane fabrication is similar in all the membranes under study, as expected, since the calculations

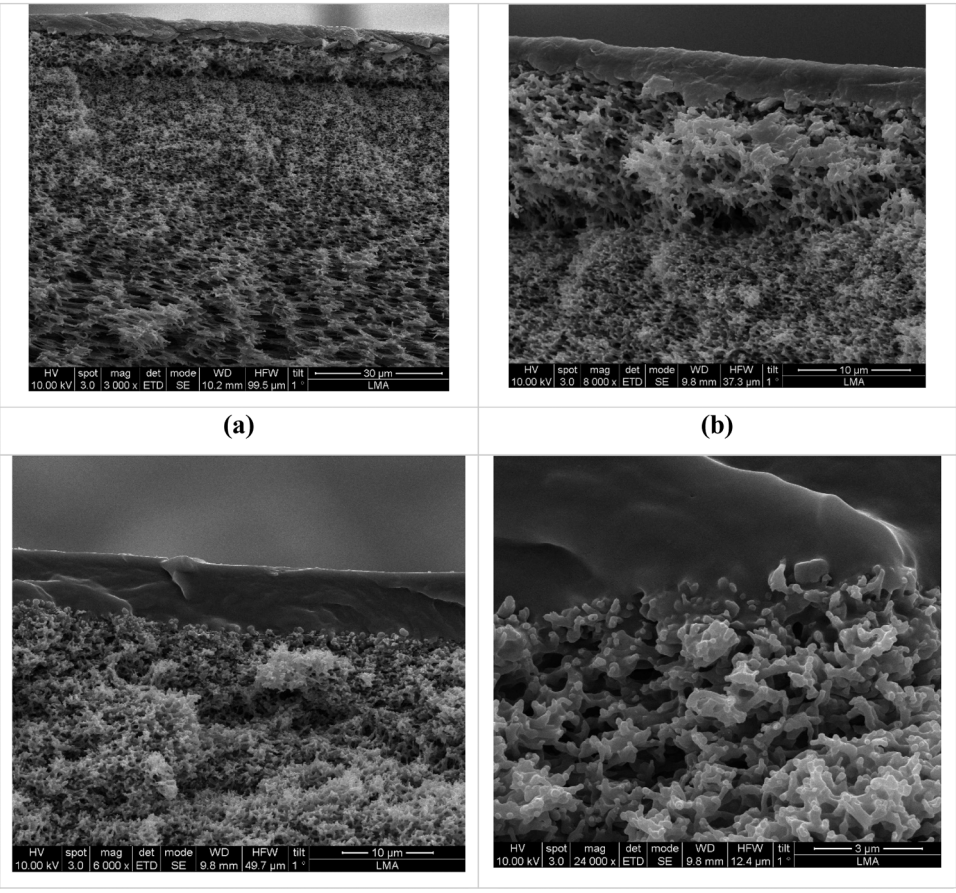

Fig. 6. SEM images of CS:ST/PES (1:1) membrane (a), 2.5 wt% zeolite 4 A/CS:ST membranes (b), both prepared from 4 wt% ST solution, and CS:ST/PES (1:1) prepared from 1 wt% ST solution (c,d).

Table 2
Gas permeation through the biopolymer composite membranes measured in the laboratory.

Membrane	Polymer matrix	Filler loading (wt%)	Active layer thickness (μm)	P (CO_2)[a] (GPU)	Selectivity (-)
Pervap4060	PDMS	0	3.25	419.7 ± 23	4.95
Zeolite 4 A	CS:CA (1:1)	0.0	29 ± 7	2.6 ± 0.0	27.8
		2.5	26 ± 12	4.5 ± 0.01	22.8
		5.0	46 ± 9	5.2 ± 0.01	29.1
Zeolite 4 A	CS:ST (1:1)	0.0	32 ± 7	137 ± 0	24.24
		2.5	40 ± 5	316 ± 1	30.7
		5.0	100 ± 0	150 ± 0	45.42

[a] The error is estimated from the measurement of two membranes.

were adapted for the same dimensions and geometry of the laboratory-scale membranes [56].

3.3. Multi-objective optimization for biogas upgrading

Fig. 8 summarize the results of the optimization of the three-stage separation process for treating a biogas effluent of 1000 $Nm^3\ h^{-1}$ as reference composed by 35/65 (v/v%) CO_2/CH_4, to achieve the product specifications set at 90 % purity and recovery of CO_2 in the permeate line (Fig. 3) while attempting to reach at least that target for the CH_4 in the retentate line. Numerical data are collected in the Supporting Information, in Tables S2 and S3 of the economical assessment.

The multi-objective optimization runs of the CO_2/CH_4 separation are focused on the selected membranes with high selectivity (2.5 wt% zeolite 4 A/CS:ST), comparable to the membranes based on zeolite 4 A/CS:CA blends, for which the optimization targets are more restrictive (95 % recovery and purity of CO_2 and CH_4 in the permeate and retentate, respectively). The pressure ratios for the operation of the membrane units considered in this study are set to 8 and 16, while the stage-cut is the decision variable, in a range of 0.05–0.95.

From the observation of results in Fig. 8**(a)** for an operation performance of the 1000 $Nm^3\ h^{-1}$ biogas treatment plant at a pressure ratio of $p/p_0 = 8$ in each membrane unit, it is highlighted that the CO_2 purity and recovery targets are reached by all the membranes under study, but the CH_4 target is not reached by the pure polymer membranes, neither the CS:ST(1:1) or the commercial fossil fuel-based PDMS membrane. The MMM loaded with the small-pore commercial zeolite 4 A achieved the highest CH_4 purity and recovery. This allowed the MMM to overcome the set target purification and recovery upon doubling the operating pressure ratio to $p/p_0 = 16$.

The lower permeability of CS:CA membranes induces a higher membrane area requirement [18], aggravating the fabrication impacts due to the acetone and acetic acid commented above seen that the flux of CS:ST blend membranes is larger than that of CS:CA blends, we speculate the cased of a hypothetical membrane with the same selectivity as the fossil-based reference PDMS membrane and a permeability larger than 20000 Barrer, provided the advancements in the research of highly porous CO_2-adsorbents [27,57] (see Figure S2 in the Supplementary information). In this case, in terms of specific costs, membrane area

Table 3
Experimental input material and energy values for the CS:CA membranes (per 1 m^2).

Membrane		CS:CA	2.5 wt% Zeolite /CS:CA	5.0 wt% Zeolite /CS:CA	Units	Data source
Synthesis of chitosan	NaOH	389.0	384.1	384.1	g	[37]
	HCl	62.30	62.18	62.18	g	
	Water	2011	1986	1986	g	
	Energy	329.6	325.4	0.325	kWh	
Zeolite 4 A (commercial)	Zeolite 4 A	0	1.029	2.058	g	This work
Cellulose acetate (commercial)	Cellulose acetate	23.15	22.86	22.57	g	This work
	Acetone	1520	1520	1520	g	This work
Membrane Fabrication	Water	1285	4279	4279	g	This work
	Acetic acid	61.74	61.74	61.74	g	This work
	PES	41.80	41.80	41.80	g	This work
	Energy	3087	3087	3.087	kWh	This work

Table 4
Experimental input material and energy values for the CS:ST membranes (per 1 m).

Membrane		CS:ST	2.5 wt% Zeolite /CS:ST	5 wt% Zeolite /CS:ST	Units	Data source
Synthesis of chitosan	NaOH	512.2	505.8	499.4	g	[37]
	HCl	82.90	81.87	81.87	g	
	Water	2648	2615	2615	g	
	Energy	433.9	428.5	0.4285	kWh	
Synthesis of starch	Water	30.86	30.48	30.10	g	[38]
	Energy	1.702	1.681	$1.66 \cdot 10^{-3}$	kWh	
Zeolite 4 A (commercial)	Zeolite 4 A	0	1.029	0.003	g	This work
Membrane Fabrication	Water	5082	5082	5082	g	This work
	Acetic acid	61.74	61.74	61.74	g	This work
	PES	41.80	41.80	41.80	g	This work
	Energy	3093	3093	3.093	kWh	This work

Table 5
Main parameters for the reference membrane.

Parameter	Value	Units	Data source
Polydimethylsiloxane	0.3	g	Sulzer
Polyacrylonitrile (intermediate support)	0.07402	g	datasheet.
Polyester interwoven fibrous support	0.1518	g	
Solvent (n-hexane)	9.7	g	
Energy	$6.01 \cdot 10^{-3}$	kWh	This work.

requirements and energy consumption, it is pointed out the technical and economic competitiveness of such a high permeability membrane makes the process viable despite the low selectivity, based on significantly low costs and membrane area requirements. In contrast, the operation at high-pressure ratios (p/p_0 =16 versus 8) favored the economic competitiveness when working with the high selectivity membrane (2.5 wt% Zeolite 4 A/CS:ST), because the greater energy consumption due to the increase of pressure ratio is highly compensated by the reduction of the required membrane area, leading to lower total costs. Therefore, the choice of the operating pressure is a key analysis to address in order to reduce the processing costs.

The process performance and calculations of specific upgrading costs as well as energy requirements in Fig. 8. The lowest specific cost was 0.31 € Nm^{-3} for the case of the zeolite 4 A/CS:CA and 0.275 € Nm^{-3} when using the Zeolite 4 A/CS:ST membrane, corresponding to a plant capacity (1000 $Nm^3\ h^{-1}$ feed), operated with a pressure ratio of 16. This cost was considered competitive when compared to the reported costs in the literature for conventional polymer-based and zeolite type membranes [58]. The energy requirements in terms of specific energy consumption results ranged 0.48–0.77 kWh Nm^{-3} (pressure ratios of 8 and 16, respectively), which strengthen the competitiveness of the multistage membrane process compared to other technologies [59].

3.4. Environmental feasibility of CS-blend membranes in biogas upgrading

In Fig. 9 the absolute environmental impacts of the CS:ST based membranes including the optimization of membrane requirement and specific energy consumption for the 1000 $Nm^3\ h^{-1}$ biogas upgrading plant optimized in **Section 3.3** are represented. Only the flows where the indicators present a value higher than 0.01 kg equivalent per functional unit are considered in the plot. Among the evaluated membranes, those blended with cellulose acetate (CS:CA) even filled with 2.5 and 5 wt% zeolite show the highest GWP values, exceeding 400 kg CO_2-eq $(Nm^3 \cdot h^{-1})^{-1}$ at 2.5 wt% loading. This is primarily attributed to their lower permeability and selectivity, which translates into significantly higher required area 159 $m^2 \cdot (Nm^3\ h^{-1})^{-1}$ than the commercial PDMS membrane. The use of acetone to dissolve the CA 1.5 wt% solution prior to blending with CS, contributes approximately 40–45 % of the total GWP. This is the reason why the energy for fabrication, particularly in the CS:CA membranes, contributes up to 30 % of the total impact, further exacerbating the environmental burden. In contrast, the 2.5 wt% zeolite A/CS:ST-PES membrane exhibit considerably lower GWP values, around 60 kg CO_2-eq $(Nm^3 \cdot h)^{-1}$),-1 closer to the commercial PDMS membrane GWP value of (10 kg CO_2-eq $(Nm^3 \cdot h^{-1})^{-1}$), due to improved membrane transport properties, which are translated into lower area requirements (Fig. 8**(a)**). For CS:ST-PES, the energy consumption upon fabrication still represents a major contributor (~45 %), but the overall impact remains moderate due to improved efficiency. The energy for operation stands out with a negligible contribution (<5 %) indicating its high potential for a future sustainable operation. Polymer matrix and the support layer contribute approximately 15–25 % of the total GWP, depending on the membrane. The incorporation of the inorganic dispersed phase is negligible at such a low loading (< 5 wt%).

As in the GWP results, the highest FD values are observed for the CS:CA-based membranes, particularly with 2.5 wt% zeolite, reaching values above 250 kg oil-eq $(Nm^3 \cdot h^{-1})^{-1}$. A major contributor to this impact category is the solvent, followed by the energy consumption upon membrane fabrication. The support and the polymer matrix contribute around 10–15 % and 10 %, respectively, while again the inorganic dispersed phase impact is negligible.

These observations are also proved by observing the total fossil resources demand, FD, of CS:ST/PES falls to 40 and 20 kg-oil $(Nm^3 \cdot h^{-1})^{-1}$,

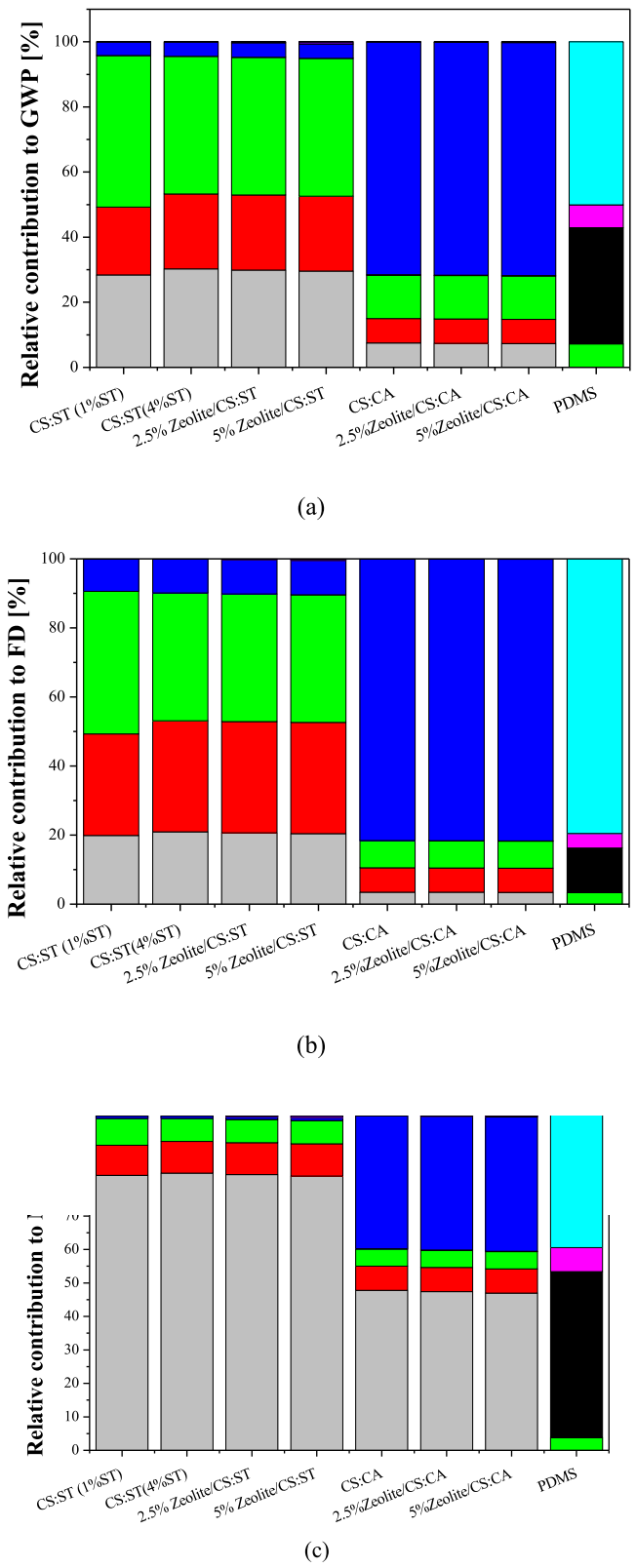

Fig. 7.. Relative contributions of the membrane fabrication to the ReCiPe midpoint indicators: (a) GWP, (b) FD, and (c) MD, respectively. Light gray, gray and black: polymers (CS, CA, PDMS); Blue and light blue: Solvents (acetic acid or n-hexane); Violet: zeolite filler; Red and magenta: support (PES or PAN+PE); Green: Energy consumption upon membrane fabrication.

at 0 and 2.5 wt% filler loading, respectively, closer to the commercial PDMS membranes (10 kg oil-eq-Nm^3 $h)^{-1}$), despite the higher permeability of the latter. In the case of CS:ST-PES, an improved membrane performance help minimize both operational and material-related burdens.

In contrast, MD contribution differs for each membrane, closely tied to material composition and performance. The dominant contributor in these systems is the polymer, which accounts for approximately 45–50 % of the total impact and CS:CA based membranes exhibit the highest MD impact. This is followed by the contributions due to the solvent used (~30 %), i.e. the acetic acid used to facilitate the dissolution in water during solution preparation and the acetone employed to dissolve the 1.5 wt% CA prior to blending with CS. Lower contributions pertain to the support layer (~10 %). The energy consumption upon fabrication represents a minor but non-negligible share (~5–8 % combined), with a slight increase observed in the zeolite-containing variants, likely due to added processing steps (Fig. 1). The filler contributes minimally in the second case (<3 %), though its role in improving selectivity and reducing operational demands may be beneficial as far as it is observed at this low loading of 2.5 – 5 wt%. In fact, the incorporation of filler into CS:CA composite membranes slightly reduces the overall MD impact (~13–14 kg Cu-eq), due to improved membrane performance that reduces the necessary active area and hence the polymer and solvent demands. Membranes based on chitosan–starch (CS:ST) show lower MD values, around 8 kg Cu-eq ($Nm^3{\cdot}h^{-1})^{-1}$, due to their moderate permeability and reduced demand of fossil derived solvent (only acetic acid for the CS dissolution because ST is dissolved in water). In fact, the major contributor to all environmental impacts for CS:ST membranes is the energy employed for starch dissolution, which requires higher temperature. while the solvent for the dissolution of CA prior to the polymer blending (see Figure S3 in the Supplementary Information.

If we observe the environmental impacts of the best membrane achieved in this work, that is, the 2.5 wt% CS:ST composite membrane with the fossil-based PDMS commercial membrane and the hypothetical membrane included in Fig. 8, considering a similar sustainable polymer blend with high permeability and low selectivity, the CS background production becomes relevant in GWP, whereas the energy and solvent devoted for membrane fabrication becomes comparable to the commercial membrane in the other environmental impacts. The impact of the gas separation is no longer negligible in comparison with the commercial membrane. This exercise highlights the observations of previous works that pointed the higher impact of permeability than selectivity on CO_2 separation performance [17]. Nevertheless, the process optimization revealed that the target objectives for biogas upgrading were hardly attained for a highly permeable, low selective membrane as for the commercial fossil-derived membrane.

4. Conclusions

This work provides an integrated experimental, multi-objective optimization, and life cycle assessment (LCA) study of membrane-based biogas upgrading. Chitosan (CS) membranes were prepared by blending with different biopolymers as starch (ST) and cellulose acetate, and hybridized by small-pore zeolite A to make mixed matrix composite membrane on compatible PES supports. The characterization revealed that the selective layer on was quite homogenous and the mechanical robustness improved by the loading ratio of zeolite particles, which showed good adhesion with the polymer matrices. The membranes performance was tested on the separation of a simulated biogas composition of 35:65 (v/v% CO_2/CH_4). The results demonstrate that membrane permeability and selectivity are critical drivers of the environmental impacts during operation. Membranes with lower transport properties, particularly the pure cellulose acetate (CS:CA) membrane, exhibited the highest environmental burdens in the three impact categories (GWP, FD, MD). This is associated with increased area and

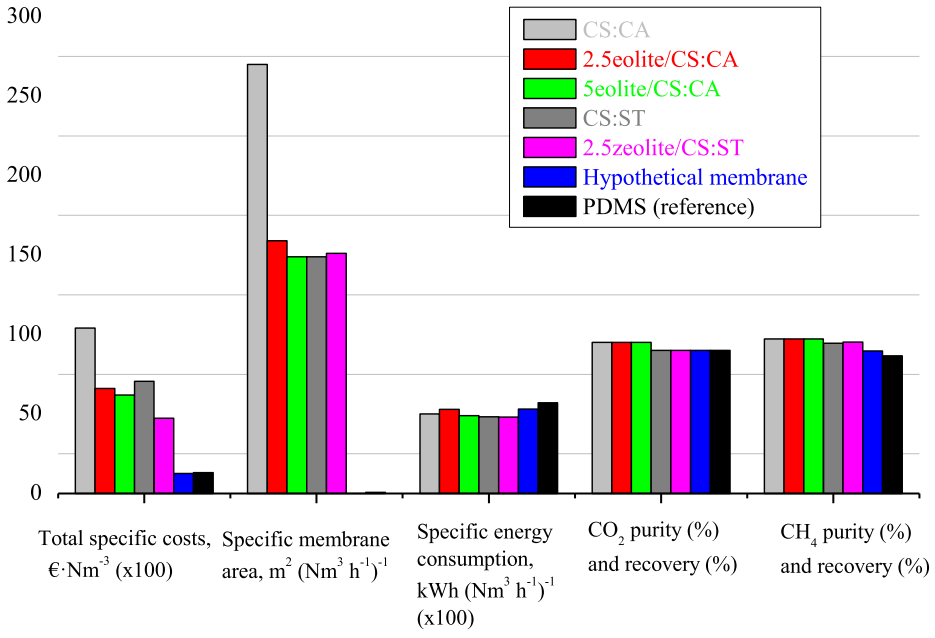

(a)

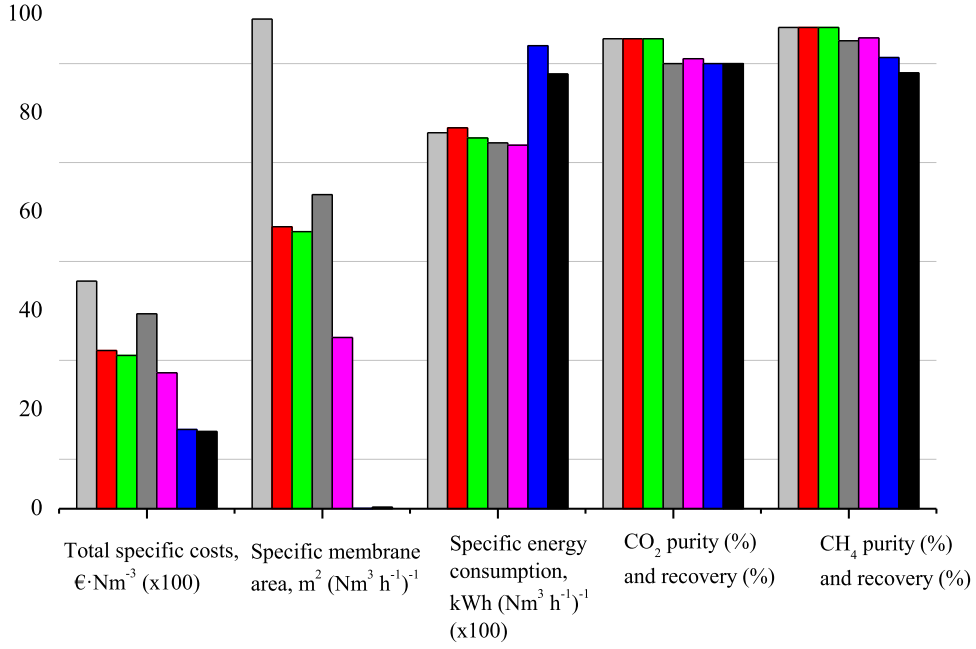

(b)

Fig. 8. Summary of the results of the multistage separation process to achieve product specifications for 90 % purity and recovery of CO_2. Plant capacity= 1000 $Nm^3 h^{-1}$: (a) p/p_0 = 4:0.5 (bar), (b) p/p_0 = 8:0.5 (bar). Light grey: CS:CA membrane, red: 5 wt% zeolite/CS:CA membrane, green: 5 wt%/CS:CA membrane; grey: CS:ST membrane, magenta: 2.5 wt% zeolite/CS:ST membrane; blue: hypothetical membrane; black: PDMS reference.

material requirements upon fabrication. The solvent choice specially emerged as a major contributor, accounting for up to one-third of the fossil and mineral resource impacts.

The incorporation of small loading of inorganic fillers (2.5–5 wt%) into CS:CA membranes slightly improved separation performance, leading to lower environmental impacts. Chitosan–starch (CS:ST) mixed matrix supported membranes improved the environmental profile of CS-based membranes, due to reduced organic solvent burden and improved transport properties that reduced both material and operational energy requirements.

High environmental impacts are not solely a function of raw material use, but are strongly driven by efficiency-related parameters such as permeability and selectivity, which are key performance parameters for reducing the area required and then, energy and solvent consumption, improving the overall sustainability of membrane-based separation processes. These findings underscore the importance of combining

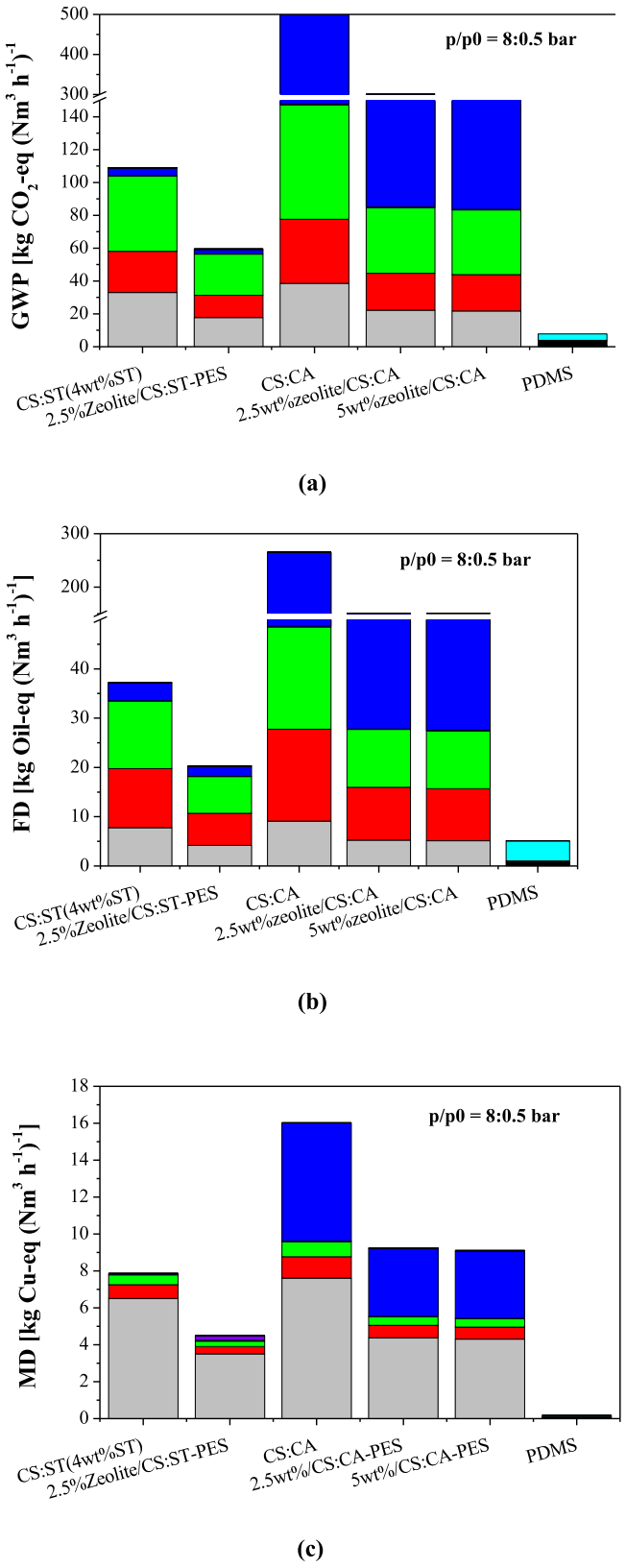

Fig. 9. GWP (a), FD (b) and MD (c) impact assessment of gas separation by membrane, for the system cradle-to-gate for a plant capacity treating 1000 Nm^3 h^{-1} biogas at $p/p_0 = 8:0.5$ pressure ratio. Light gray, gray and black: polymers (CS, CA or PDMS); Blue or light blue: Solvents (acetic acid or n-hexane); Violet: zeolite filler; Red and magenta: support (PES or PAN+PE); Green: Energy consumption upon membrane fabrication; Yellow: energy consumption upon gas separation.

material innovation (e.g., high-performance polymers, fillers [57] and green solvents [16,60]) with process optimization (e.g., solvent recovery, reduced membrane thickness) to develop sustainable membrane systems for gas separation applications.

Nomenclature

A	Effective membrane area for permeation (cm^2)
ACI	Acidification
AD	Abiotic depletion
AP	Acidification
ATR-FTIR	Attenuated Total Reflectance Fourier-Transform Infrared Spectroscopy
BSCF	Oxide perovskite
CA	Cellulose acetate
CC	Climate change
CCU	Carbon capture and utilization
CED	Cumulative energy demand
CS	Chitosan
CH_4	Methane
CO_2	Carbon dioxide
C_p	Specific heat capacity of the main solvent ($J\ kg^{-1}{\cdot}K^{-1}$)
d	Impeller diameter (m)
ECFM	Ecotoxicity, marine
EP	Eutrophication
EQ	Ecosystem quality
ETS-10	Microporous titanosilicate
ERDP	Energy resource depletion potential
EU	Eutrophication
EUF	Eutrophication, freshwater
EUM	Eutrophication, marine
EUT	Eutrophication, terrestrial
FAEP	Freshwater aquatic ecotoxicity
FD	Fossil fuel depletion
FU	Functional unit
GWP	Global warming potential
HCl	Hydrochloric acid
HH	Human health
HTC	Human toxicity, carcinogenic
HTNC	Human toxicity, non-carcinogenic
HTTP	Human toxicity
H_2O	Water
ISO	International organization for standardization
LCA	Life cycle assessment
LCI	Life cycle inventory
LCIA	Life cycle impact assessment
LU	Land use
MAEP	Marine aquatic ecotoxicity
MD	Material depletion
MMM	Mixed matrix membrane
MRD	Mineral resources use
MRDP	Energy resource depletion potential
m_{mix}	Mass of the mixture (kg)
m_{liq}	Mass of liquid of the solution (kg)
m_{vap}	Mass of the liquid that is evaporated (kg)
NaOH	Sodium hidroxide
NREU	Non-renewable energy
N	rotational speed of the agitator (s^{-1})
N_p	Power dimensionless number
N_2	Nitrogen
P	Intrinsic permeability of the membrane for each gas (cm^3(STP) cm cm^{-2} $cmHg^{-1}$ s^{-1}).
PAN	Polyacrylonitrile
PDMS	Polydimethylsiloxane
PES	Polyethersulfone
PIM-1	Intrinsic Microporous Polymer 1

POP	Photochemical oxidation
PVA	Polyvinyl alcohol
PVIM	Polyvinylimidazole
p_p	permeate pressure (cmHg)
p_r	retentate pressure (cmHg)
Q_{dry}	Heat necessary for drying (J)
Q_{heat}	Energy to reach the set point temperature (J)
RD	Resource depletion
RINP	Respiratory inorganics
SEM	Scanning electron microscopy
S.F	Separation factor, Eq. (3).
ST	Starch
t	Time duration for the stirring process (s)
TECP	Terrestrial ecotoxicity
TGA	Thermogravimetric analysis
THF	Tetrahydrofuran
T_{boil}	Boiling temperature of the liquid (K)
T_r	Heating temperature (K)
T_0	Starting temperature (K)
UF	Ultrafiltration
UiO-66-NH_2	Metal organic framework (MOF) University of Oslo 66
V_{mix}	Volume of the mixture (cm^3)
WU	Water use
XRD	X-ray diffraction
α	Ideal Selectivity, Eq. (2).
δ	Membrane thickness (cm)
ρ_{mix}	Density of the mixture (g cm^{-3})
η_{dry}	Drying efficiency
η_{stir}	Efficiency of the stirring
ΔH_{vap}	Evaporation enthalpy of water (J $kg^{-1}{\cdot}K^{-1}$)
p/p_0	Pressure ratio

CRediT authorship contribution statement

Marta Rumayor: Writing – review & editing, Writing – original draft, Visualization, Validation, Supervision, Project administration, Methodology, Investigation, Formal analysis, Conceptualization. **Carlos Téllez:** Writing – review & editing, Writing – original draft, Visualization, Validation, Resources, Methodology, Investigation, Funding acquisition, Data curation. **Clara Casado-Coterillo:** Writing – review & editing, Writing – original draft, Visualization, Resources, Project administration, Methodology, Investigation, Funding acquisition, Formal analysis, Conceptualization. **Aurora Garea:** Writing – review & editing, Visualization, Validation, Methodology, Investigation, Formal analysis, Conceptualization. **Beheshta Dawood:** Writing – original draft, Validation, Methodology, Investigation, Data curation, Conceptualization. **Cristina Pina-Vidal:** Visualization, Validation, Investigation, Formal analysis, Data curation. **Andrea Torre-Celeizabal:** Validation, Methodology, Investigation, Formal analysis, Data curation.

Declaration of Competing Interest

The authors declare that they have no known competing financial interests or personal relationships that could have appeared to influence the work reported in this paper.

Acknowledgements

Funding from regional government through "Contrato Programa Gobierno de Cantabria – UC", the European Union for the Bio4HUMAN GA 101135144 Horizon Europe project and the Spanish State Research Agency for the project grant PID2019-108136RB-C31/AEI/10.13039/501100011033 are gratefully acknowledged. A.T.C. also acknowledges the AEI for the Early-Stage Researcher contract PRE2020-09765/aei/10.13039/50111000110333. Grant PID2022-138582OB-I00 funded by MICIU/AEI/10.13039/501100011033 and ERDF/EU is also recognized. Authors acknowledge the use of instrumentation as well as the technical advice provided by the National Facility ELECMI ICTS, "Laboratorio de Microscopías Avanzadas" node at the University of Zaragoza.

Appendix A. Supporting information

Supplementary data associated with this article can be found in the online version at doi:10.1016/j.jece.2025.117688.

Data availability

Data will be made available on request.

References

[1] Iliuta Intensified processes for CO_2 capture and valorization by catalytic conversion, Chem. Eng. Process. - Process Intensif. 205 (2024) 109995. https://doi.org/10.1016/j.cep.2024.109995.
[2] W.R. Stahel, Circular economy, Nature 531 (2016) 435–438, https://doi.org/10.1038/531435a.
[3] W. Xie, T. Li, A. Tiraferri, E. Drioli, A. Figoli, J.C. Crittenden, B. Liu, Toward the next generation of sustainable membranes from green chemistry principles, ACS Sustain. Chem. Eng. 9 (2021) 50–75, https://doi.org/10.1021/acssuschemeng.0c07119.
[4] S.I. Voicu, V.K. Thakur, Green polymers-based membranes for water reuse in a circular economy context, Curr. Opin. Green. Sustain. Chem. 43 (2023) 100852, https://doi.org/10.1016/j.cogsc.2023.100852.
[5] F. Russo, F. Galiano, A. Iulianelli, A. Basile, A. Figoli, Biopolymers for sustainable membranes in CO_2 separation: a review, Fuel Process. Technol. 213 (2021) 106643, https://doi.org/10.1016/j.fuproc.2020.106643.
[6] R. Salvador, M.V. Barros, M. Pieroni, D.A. Lopes Silva, F. Freire, A.C. De Francisco, Overarching business models for a circular bioeconomy: systematising archetypes, Sustain. Prod. Consum 43 (2023) 349–362, https://doi.org/10.1016/j.spc.2023.11.010.
[7] L. Matesanz-Niño, J. Moranchel-Perez, C. Álvarez, A.E. Lozano, C. Casado-Coterillo, Mixed matrix membranes using porous organic polymers (POPs)—Influence of textural properties on CO_2/CH_4 separation, Polym. (Basel) 15 (2023) 4135–4157, https://doi.org/10.3390/polym15204135.
[8] C. Casado-Coterillo, A. Fernández-Barquín, B. Zornoza, C. Téllez, J. Coronas, Á. Irabien, Synthesis and characterisation of MOF/ionic liquid/chitosan mixed matrix membranes for CO_2/N_2 separation, RSC Adv. 5 (2015) 102350–102361, https://doi.org/10.1039/c5ra19331a.
[9] K. Papchenko, E. Ricci, M.G. De Angelis, Modelling across multiple scales to design biopolymer membranes for sustainable gas separations: 1—atomistic approach, Polym. (Basel) 15 (2023) 1805–1820, https://doi.org/10.3390/polym15071805.
[10] S. Sala, E. Crenna, M. Secchi, E. Sanyé-Mengual, Environmental sustainability of European production and consumption assessed against planetary boundaries, J. Environ. Manag. 269 (2020) 110686, https://doi.org/10.1016/j.jenvman.2020.110686.
[11] K. Archana, A.S. Viskram, P.Senthil Kumar, S. Manikandan, A. Saravanan, L. Natrayan, A review on recent technological breakthroughs in anaerobic digestion of organic biowaste for biogas generation: Challenges towards sustainable development goals, Fuel 358 (2024) 130298, https://doi.org/10.1016/j.fuel.2023.130298.
[12] E. Zschieschang, P. Pfeifer, L. Schebek, Life cycle assessment in chemical and micro reaction engineering, Chem. Eng. Technol. 36 (2013) 911–920, https://doi.org/10.1002/ceat.201200635.
[13] W.H.D. Goh, H.S. Lau, W.F. Yong, An integrated life cycle assessment and techno-economic analysis: Evaluation on the production of polymers of intrinsic microporosity (PIM-1) and UiO-66-NH_2 as membrane materials, Sci. Total Environ. 892 (2023) 164582, https://doi.org/10.1016/j.scitotenv.2023.164582.
[14] R. Abejon, A. Torre-celeizabal, C. Casado-coterillo, A. Garea, Analysis of the techno-economic competitiveness of a three-stage membrane separation process for biogas upgrading using a biopolymer-based mixed-matrix membrane, ACS Sustain. Chem. Eng. 12 (2024) 1297–1308, https://doi.org/10.1021/acsuschemeng.3c06676.
[15] H.Y. Nguyen Thi, S. Kim, B.T. Duy Nguyen, D. Lim, S. Kumar, H. Lee, G. Szekely, J. F. Kim, Closing the sustainable life cycle loop of membrane technology via a cellulose biomass platform, ACS Sustain. Chem. Eng. 10 (2022) 2532–2544, https://doi.org/10.1021/acssuschemeng.1c08554.
[16] A. Torre-Celeizabal, F. Russo, F. Galiano, A. Figoli, C. Casado-Coterillo, A. Garea, Green synthesis of cellulose acetate mixed matrix membranes: Structure – Function Characterization, ACS Sustain. Chem. Eng. 13 (2025) 1253–1270, https://doi.org/10.1021/acssuschemeng.4c07538.
[17] I. Echarri, C. Casado-Coterillo, M. Rumayor, A. Navajas, L.M. Gandía, Environmental impact improvement of chitosan-based mixed-matrix membranes manufacture for CO_2 gas separation by life cycle assessment, Chem. Eng. Technol. 46 (2023) 2184–2191, https://doi.org/10.1002/ceat.202200397.
[18] L. Tock, F. Maréchal, Life cycle assessment based process design of CO_2 capture options, Comput. Aided Chem. Eng. 33 (2014) 1033–1038, https://doi.org/10.1016/B978-0-444-63455-9.50007-6.

[19] T. Eljaddi, L. Giordano, D. Roizard, Towards the synthesis of greener membranes: Interest of PVA as porous support for membrane application in gas and liquid separations, Sep. Purif. Technol. 263 (2021) 118357, https://doi.org/10.1016/j.seppur.2021.118357.
[20] S. Bello, P. Méndez-Trelles, E. Rodil, G. Feijoo, M.T. Moreira, Towards improving the sustainability of bioplastics: Process modelling and life cycle assessment of two separation routes for 2,5-furandicarboxylic acid, Sep. Purif. Technol. 233 (2020) 116056, https://doi.org/10.1016/j.seppur.2019.116056.
[21] P. Luis, A. Amelio, S. Vreysen, V. Calabro, B. Van der Bruggen, Simulation and environmental evaluation of process design: Distillation vs. hybrid distillation-pervaporation for methanol/tetrahydrofuran separation, Appl. Energy 113 (2014) 565–575, https://doi.org/10.1016/j.apenergy.2013.06.040.
[22] N. Attari, R. Hausler, Cradle-to-gate life cycle assessment of cellulose-based membrane manufacturing process, Int. J. Environ. Pollut. Remediat 11 (2023) 20–31, https://doi.org/10.11159/ijepr.2023.003.
[23] P. Markewitz, J. Marx, A. Schreiber, P. Zapp, Ecological evaluation of coal-fired oxyfuel power plants -Cryogenic versus membrane-based air separation, Energy Procedia 37 (2013) 2864–2876, https://doi.org/10.1016/j.egypro.2013.06.172.
[24] E. Khaki, H. Abyar, M. Nowrouzi, H. Younesi, M. Abdollahi, M.G. Enderati, Comparative life cycle assessment of polymeric membranes: Polyacrylonitrile, polyvinylimidazole and poly (acrylonitrile-co-vinylimidazole) applied for CO_2 sequestration, Environ. Technol. Innov. 22 (2021) 101507, https://doi.org/10.1016/j.eti.2021.101507.
[25] R. Liu, T.R. Alsenani, J. Kumar, N.A. Othman, H.S. Majdi, A.T. Hoang, S.B. Moussa, N.D.K. Pham, Effect of O_2 transport membrane and CO_2 capture membranes on the performance of the biomass-based power generation: An artificial intelligence based multi-objective optimization and techno-economic and environmental evaluatio, Sep. Purif. Technol. 323 (2023) 124401, https://doi.org/10.1016/j.seppur.2023.124401.
[26] L. Giordano, D. Roizard, E. Favre, Life cycle assessment of post-combustion CO_2 capture: a comparison between membrane separation and chemical absorption processes, Int. J. Greenh. Gas. Control 68 (2018) 146–163, https://doi.org/10.1016/j.ijggc.2017.11.008.
[27] H. Luo, F. Cheng, L. Huelsenbeck, N. Smith, Comparison between conventional solvothermal and aqueous solution-based production of UiO-66-NH_2: life cycle assessment, techno-economic assessment, and implications for CO_2 capture and storage, J. Environ. Chem. Eng. 9 (2021) 105159, https://doi.org/10.1016/j.jece.2021.105159.
[28] F. Prézélus, L. Tiruta-Barna, C. Guigui, J.C. Remigy, A generic process modelling – LCA approach for UF membrane fabrication: Application to cellulose acetate membranes, J. Membr. Sci. 618 (2021) 118594, https://doi.org/10.1016/j.memsci.2020.118594.
[29] R. Abejón, C. Casado-Coterillo, A. Garea, Techno-economic optimization of multistage membrane processes with Innovative hollow fiber modules for the production of high-purity CO_2 and CH_4 from different sources, Ind. Eng. Chem. Res. 61 (2022) 8149–8165, https://doi.org/10.1021/acs.iecr.2c01138.
[30] C.V. Funk, D.R. Lloyd, Zeolite-filled microporous mixed matrix (ZeoTIPS) membranes: prediction of gas separation performance, J. Membr. Sci. 313 (2008) 224–231, https://doi.org/10.1016/j.memsci.2008.01.002.
[31] G. Valenti, A. Arcidiacono, J.A. Nieto Ruiz, Assessment of membrane plants for biogas upgrading to biomethane at zero methane emission, Biomass.. Bioenergy 85 (2016) 35–47, https://doi.org/10.1016/j.biombioe.2015.11.020.
[32] R. Borgohain, U. Pattnaik, B. Prasad, B. Mandal, A review on chitosan-based membranes for sustainable CO_2 separation applications: mechanism, issues, and the way forward, Carbohydr. Polym. 267 (2021) 118178, https://doi.org/10.1016/j.carbpol.2021.118178.
[33] A. Torre-Celeizabal, C. Casado-Coterillo, A. Gomis-Berenguer, J. Iniesta, A. Garea, Chitosan-based mixed matrix composite membranes for CO_2/CH_4 mixed gas separation. Experimental characterization and performance validation, Sep. Purif. Technol. 325 (2023) 124535, https://doi.org/10.1016/j.seppur.2023.124535.
[34] ISO 14040, 2006 Environmental management life cycle assessment principles and framework, Int. Organ. Stand (2006) 20. ⟨https://www.iso.org/standard/37456.html⟩ (accessed November 22, 2022).
[35] ISO 14044, 2006 Environmental management life cycle assessment: requirements and guidelines, Int. Organ. Stand (2006) 49. ⟨https://www.iso.org/standard/38498.html⟩ (accessed November 22, 2022).
[36] A. Hosney, S. Ullah, K. Barčauskaitė, A review of the chemical extraction of chitosan from shrimp wastes and prediction of factors affecting chitosan yield by using an artificial neural network, Mar. Drugs 20 (2022) 675–694, https://doi.org/10.3390/md20110675.
[37] F. Ben Amara, M. Bouzid, M. Sahnoun, Y. Ben Nasr, B. Jaouadi, S. Bejar, S. Jemli, Valorization of potato peels starch for efficient β-cyclodextrin production and purification through an eco-friendly process, Starch/Staerke 74 (1–8) (2022) 2200037, https://doi.org/10.1002/star.202200037.
[38] G. Wernet, C. Bauer, B. Steubing, J. Reinhard, E. Moreno-Ruiz, B. Weidema, The ecoinvent database version 3 (part I): overview and methodology, Int. J. Life Cycle Assess. 21 (2016) 1218–1230.
[39] F. Piccinno, R. Hischier, S. Seeger, C. Som, From laboratory to industrial scale: a scale-up framework for chemical processes in life cycle assessment studies, J. Clean. Prod. 135 (2016) 1085–1097, https://doi.org/10.1016/j.jclepro.2016.06.164.
[40] National_Institute_for_Public_Health_and_the_Environment, LCIA: the ReCiPe model, ⟨Https://Www.Rivm.Nl/En/Life-Cycle-Assessment-Lca/Recipe⟩ (2020).
[41] GreenDelta, OpenLCA 2.3, ⟨Https://www.openlca.org⟩ (2024). (Last accessed june 2025).
[42] A. Torre-Celeizabal, C. Casado-Coterillo, R. Abejón, A. Garea, Simultaneous production of high-quality CO_2 and CH_4 via multistage process using chitosan-based membranes, Sep. Purif. Technol. 320 (2023) 124050, https://doi.org/10.1016/j.seppur.2023.124050.
[43] M.R. Bussieck, A. Meeraus, General Algebraic Modeling System (GAMS), in: J. Kallrath (Ed.), Model. Lang. Math. Optim. Appl. Optim, Springer, Boston, MA, 2004, p. 137, https://doi.org/10.1007/978-1-4613-0215-5_8.
[44] I.E. Grossmann. Advanced Optimization for Process Systems Engineering, 1st ed., Cambridge University Press, Padstow Cornwall, UK, 2021, p. 206, https://doi.org/10.1017/9781108917834.
[45] H.G. Premakshi, K. Ramesh, M.Y. Kariduraganavar, Modification of crosslinked chitosan membrane using NaY zeolite for pervaporation separation of water-isopropanol mixtures, Chem. Eng. Res. Des. 94 (2015) 32–43, https://doi.org/10.1016/j.cherd.2014.11.014.
[46] B.A. Alimi, M. Hoque, S. Pathania, J. Wilson, B. Duffy, J.M. Celayeta Frias, Structural, thermal, optical, and mechanical properties of composite films developed from the button mushroom (*Agaricus bisporus*)-sourced high molecular weight chitosan and potato starch, Lwt 185 (2023) 115201, https://doi.org/10.1016/j.lwt.2023.115201.
[47] J. Wang, X. Zheng, H. Wu, B. Zheng, Z. Jiang, X. Hao, B. Wang, Effect of zeolites on chitosan/zeolite hybrid membranes for direct methanol fuel cell, J. Power Sources 178 (2008) 9–19, https://doi.org/10.1016/j.jpowsour.2007.12.063.
[48] J. Ahmad, M.B. Hägg, Effect of zeolite preheat treatment and membrane post heat treatment on the performance of polyvinyl acetate/zeolite 4A mixed matrix membrane, Sep. Purif. Technol. 115 (2013) 163–171, https://doi.org/10.1016/j.seppur.2013.04.050.
[49] A. Fernández-Barquín, R. Rea, D. Venturi, M. Giacinti-Baschetti, M.G. De Angelis, C. Casado-Coterillo, Á. Irabien, Effect of relative humidity on the gas transport properties of zeolite A/PTMSP mixed matrix membranes, RSC Adv. 8 (2018) 3536–3546, https://doi.org/10.1039/c7ra13039b.
[50] A. Fernández-Barquín, C. Casado-Coterillo, M. Palomino, S. Valencia, A. Irabien, LTA/poly(1-trimethylsilyl-1-propyne) mixed-matrix membranes for high-temperature CO_2/N_2 separation, Chem. Eng. Technol. 38 (2015) 658–666, https://doi.org/10.1002/ceat.201400641.
[51] M. Galizia, W.S. Chi, Z.P. Smith, T.C. Merkel, R.W. Baker, B.D. Freeman, 50th anniversary perspective: Polymers and mixed matrix membranes for gas and vapor separation: a review and prospective opportunities, Macromolecules 50 (2017) 7809–7843, https://doi.org/10.1021/acs.macromol.7b01718.
[52] P. Fronza, A.L.R. Costa, A.S. Franca, L.S. de Oliveira, Extraction and characterization of starch from cassava peels, Starch/Staerke 75 (2023) 1–8, https://doi.org/10.1002/star.202100245.
[53] W. Lawler, J. Alvarez-Gaitan, G. Leslie, P. Le-Clech, Comparative life cycle assessment of end-of-life options for reverse osmosis membranes, Desalination 357 (2015) 45–54, https://doi.org/10.1016/j.desal.2014.10.013.
[54] J.M.F. Pavoni, C.L. Luchese, I.C. Tessaro, Impact of acid type for chitosan dissolution on the characteristics and biodegradability of cornstarch/chitosan based films, Int. J. Biol. Macromol. 138 (2019) 693–703, https://doi.org/10.1016/j.ijbiomac.2019.07.089.
[55] P. Ortiz-Albo, V.D. Alves, I. Kumakiri, J. Crespo, L.A. Neves, A greener route to prepare PEBAX®1074 membranes for gas separation processes, J. Membr. Sci. 693 (2024) 122346, https://doi.org/10.1016/j.memsci.2023.122346.
[56] T.M.T. Nguyen, J.W. Chen, M.T. Pham, H.M. Bui, C.C. Hu, S.J. You, Y.F. Wang, A high-performance ZIF-8 membrane for gas separation applications: synthesis and characterization, Environ. Technol. Innov. 31 (2023) 103169, https://doi.org/10.1016/j.eti.2023.103169.
[57] C. Pina-Vidal, V. Berned-Samatán, E. Piera, M.Á. Caballero, C. Téllez, Mechanochemical encapsulation of caffeine in UiO-66 and UiO-66-NH_2 to obtain polymeric composites by extrusion with recycled polyamide 6 or polylactic acid biopolymer, Polym. (Basel) 16 (2024) 637–666, https://doi.org/10.3390/polym16050637.
[58] J. Gascon, F. Kapteijn, B. Zornoza, V. Sebastián, C. Casado, J. Coronas, Practical approach to zeolitic membranes and coatings: State of the art, opportunities, barriers, and future perspectives, Chem. Mater. 24 (2012) 2829–2844, https://doi.org/10.1021/cm301435j.
[59] P. Gkotsis, P. Kougias, M. Mitrakas, A. Zouboulis, Biogas upgrading technologies – recent advances in membrane-based processes, Int. J. Hydrog. Energy 48 (2023) 3965–3993, https://doi.org/10.1016/j.ijhydene.2022.10.228.
[60] J.M.F. Pavoni, N.Z. dos Santos, I.C. May, L.D. Pollo, I.C. Tessaro, Impact of acid type and glutaraldehyde crosslinking in the physicochemical and mechanical properties and biodegradability of chitosan films, Polym. Bull. 78 (2021) 981–1000, https://doi.org/10.1007/s00289-020-03140-4.